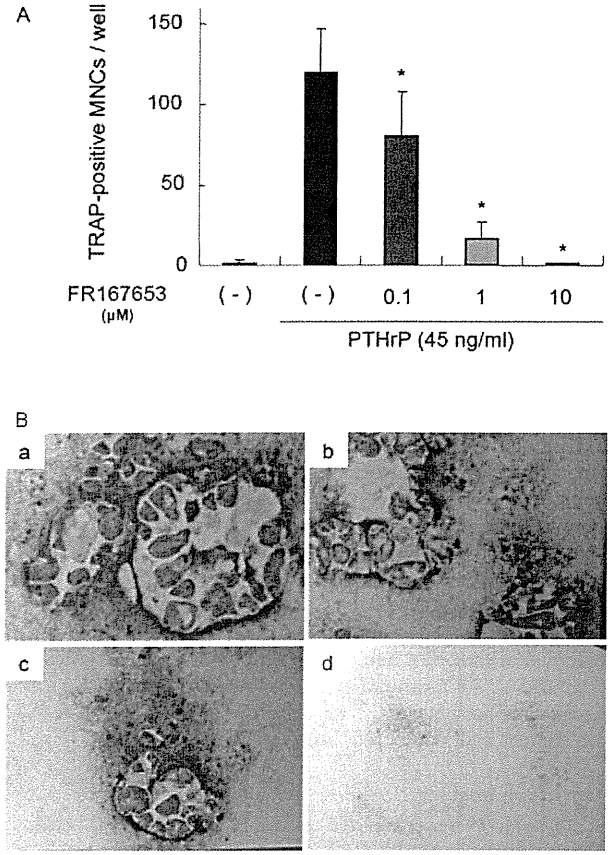

Figure 2. FR167653 inhibits TRAP-positive osteoclast formation in PTHrP-treated bone marrow cells. A. Bone marrow cells were treated with PTHrP (45 ng/ml) and FR167653 for six days. TRAP-positive MNCs with three or more nuclei were counted as osteoclasts. n = 9. *: $p<0.001$ versus the group treated only with PTHrP. B. TRAP staining for bone marrow cells stimulated with PTHrP (45 ng/ml). a: no treatment. b: FR167653 (0.1 μM). c: FR167653 (1 μM). d: FR167653 (10 μM). TRAP-positive MNCs appear as red cells with clear peripheries.
doi:10.1371/journal.pone.0023199.g002

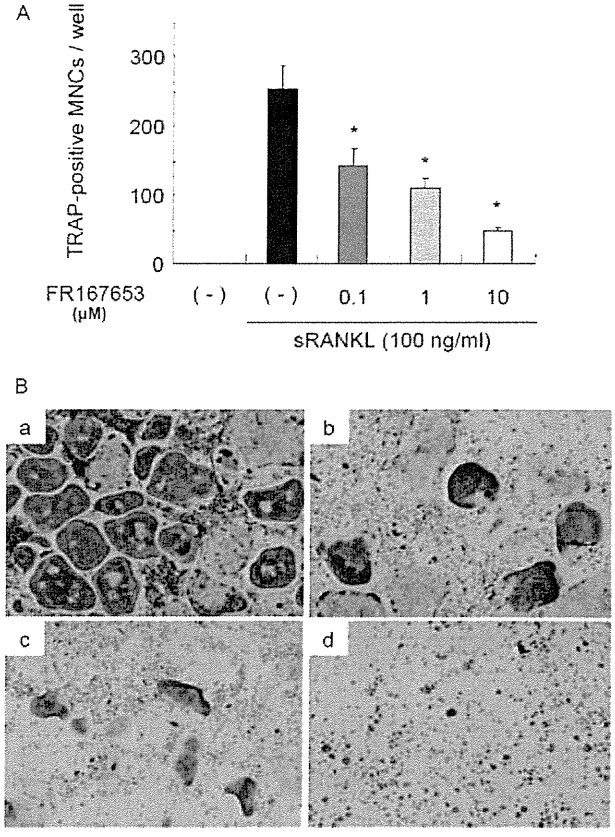

Figure 3. Effects of FR167653 on osteoclast formation in M-CSF-dependent bone marrow macrophages treated with sRANKL. A. Osteoclast formation assay using M-CSF-dependent bone marrow macrophages (MDBMMs) prepared as described in the Materials and Methods section. TRAP-positive MNCs with three or more nuclei were counted as osteoclasts. n = 6. *: $p<0.001$ versus the group treated only with sRANKL. B. TRAP staining for MDBMMs stimulated by sRANKL (100 ng/ml). a: No treatment. b: FR167653 (0.1 μM). c: FR167653 (1 μM). d: FR167653 (10 μM).
doi:10.1371/journal.pone.0023199.g003

Bone marrow stromal cells were obtained by culturing primary bone marrow cells for ten days. Almost all non-adherent or loosely attached hematopoietic cells in the primary bone marrow cell cultures were removed by pipetting each time when the medium was changed. Expression of RANKL and OPG mRNA in bone marrow stromal cells was increased or decreased, respectively, within three days of PTHrP treatment. The increased expression even lasted 6 days post-treatment. Even at a dose of 10 μM, FR167653 has no detectable effect on the PTHrP-mediated expression of RANKL and OPG mRNA (Figure 4). Taken together, these results further suggest that FR167653 acts directly on osteoclast precursors (rather than on stromal cells or osteoblasts) in its role as an inhibitor of osteoclast formation.

Expression of c-Fos and NFATc1 in osteoclast precursors (MDBMMs) were inhibited by FR167653

In order to investigate the mechanism of FR167653 on osteoclast formation in osteocalst precursor cells, we detected the expression of c-Fos and NFATc1 in bone marrow macrophage cells by western blotting and RT-PCR following the FR167653 treatments. As shown in Figure 5, the mRNA expression levels of c-fos and NFATc1 were dramatically increased when treated with sRANKL and these effects were inhibited by FR167653 in a dose-dependent manner($p<0.05$; Figure 5A). Similarly, c-Fos and NFATc1 protein levels were decreased in the presence of FR167653 dose-dependently (Figure 5B).

FR167653 reduces PTHrP-induced bone resorption in vivo

We next examined the effects of FR167653 on PTHrP-induced bone resorption *in vivo*. Animal models of bone resorption were established by direct injection of PTHrP onto the dorsal surface of mice calvaria. Radiographic evidence of bone resorption comprises zones of increased radiolucency in the calvaria. Histologically, these changes are associated with significant periosteal bone resorption on the dorsal calvarial surface and increased marrow spaces, accompanied with increased numbers of osteoclasts. FR167653 significantly reduced the radiographic bone resorption areas ($p<0.05$; Figure 6) and osteoclast number (as determined on histological sections) ($p<0.005$, Figure 7).

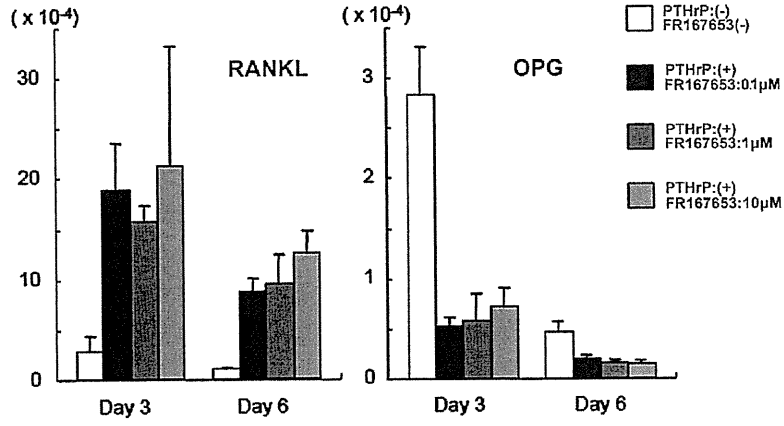

Figure 4. FR167653 does not affect OPG or RANKL expression by PTHrP-treated stromal cells. Bone marrow stromal cells were seeded into six-well plates and treated with PTHrP (90 ng/ml) and FR167653 at various concentrations for three and six days. Real-time PCR was used to determine the OPG or RANKL gene expression levels. The results are shown as mean ±S.D. of three independent experiments. Expression of RANKL and OPG mRNA was increased or decreased, respectively, within three days of PTHrP treatment, and lasted 6 days post-treatment. The expression level of RANKL and OPG did not changed by adding 1 μM or 10 μM FR167653 ($P>0.05$).
doi:10.1371/journal.pone.0023199.g004

Treatment with FR167653 has the effect on the cotnrol of PTHrP-induced systemic hypercalcemia

PTHrP is one of the causative factors of the hypercalcemia that is associated with malignancy, since PTHrP can induce systemic bone resorption. Furthermore, extensive local bone resorption is to some extent a contributory cause of hypercalcemia. For this reason, we monitored whole-blood ionized calcium levels in our experimental system. The level of whole-blood ionized calcium was increased at three hours after PTHrP injection on days 3 and 5 compared to day 1. When additionally treated with FR167653, the whole-blood ionized calcium concentration was significantly decreased at day 3, but not day 5. This suggest the functional involvement of p38 MAPK in PTHrP-induced systemic hypercalcemia (Figure 8).

Discussion

There are several reports about p38 MAPK inhibitor, SB203580, inhibits osteoclast differentiation in RAW264 induced by RANKL [28] or in bone marrow cells induced by 1α, 25-$(OH)_2$ D_3 and prostaglandin E_2 (PGE_2) [14]. Previously, we reported that M-CSF-dependent sRANKL- and TNFα-induced osteoclast formation in primary bone marrow cells, and collagen-induced arthritis in rats were inhibited by FR167653 [23]. Here we further show that FR167653, a selective inhibitor of p38 MAPK, strongly inhibits osteoclast differentiation in PTHrP-treated bone marrow cell cultures.

We also investigated the mechanism of FR167653 involved in the inhibition of osteoclast formation. Most osteoclastgenesis inducers are thought to stimulate osteoclast formation via up-

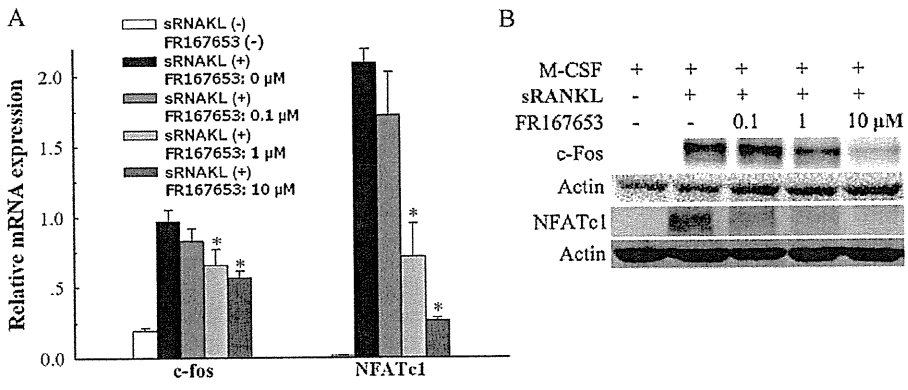

Figure 5. The effects of FR167653 on sRANKL-induced c-Fos and NFATc1 expression level in M-CSF-dependent bone marrow macrophages (MDBMMs). Bone marrow macrophages were treated with 100 ng/ml M-CSF and 100 ng/ml sRANKL without or with FR67653 at the indicated concentration. After 24 h incubation, cells were harvested and subjected to RT-PCR (A). For western blot analysis (B), the cells were incubated for 48 h. Expression of c-Fos and NFATc1 in both mRNA and protein levels were increased following the sRANKL treatment. This enhancement was inhibited by FR167653 in a dose dependent manner. The results are shown as mean ±S.D. of three independent experiments. *: $p<0.05$ versus the group treated only with sRANKL.
doi:10.1371/journal.pone.0023199.g005

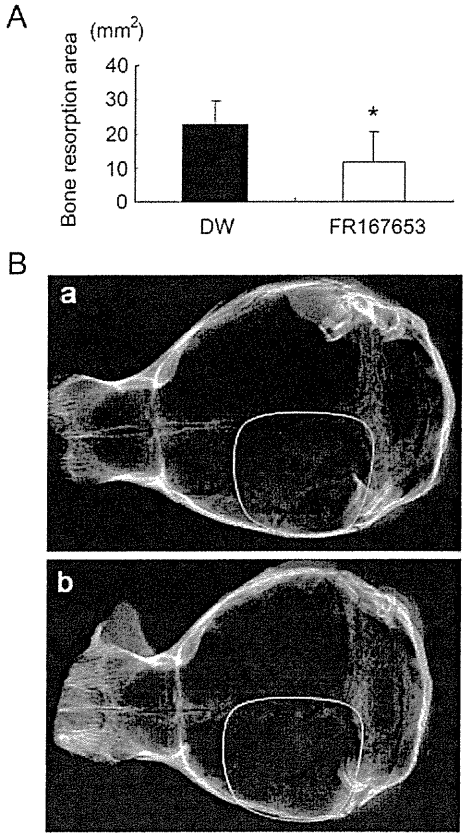

Figure 6. The effect of FR167653 on PTHrP-induced bone resorption. The calvarial bone resorption was measured radiographically on the left side (area marked by yellow line) where treated by direct subcutaneous injection of PTHrP. A. Treatment by FR167653 reduced the bone resorption area (*: P<0.005). DW:distilled water. B. Representative X-rays of mouse calvaria with PTHrP-induced bone resorption. a: control group (treated with DW). b: FR167653 treatment group.
doi:10.1371/journal.pone.0023199.g006

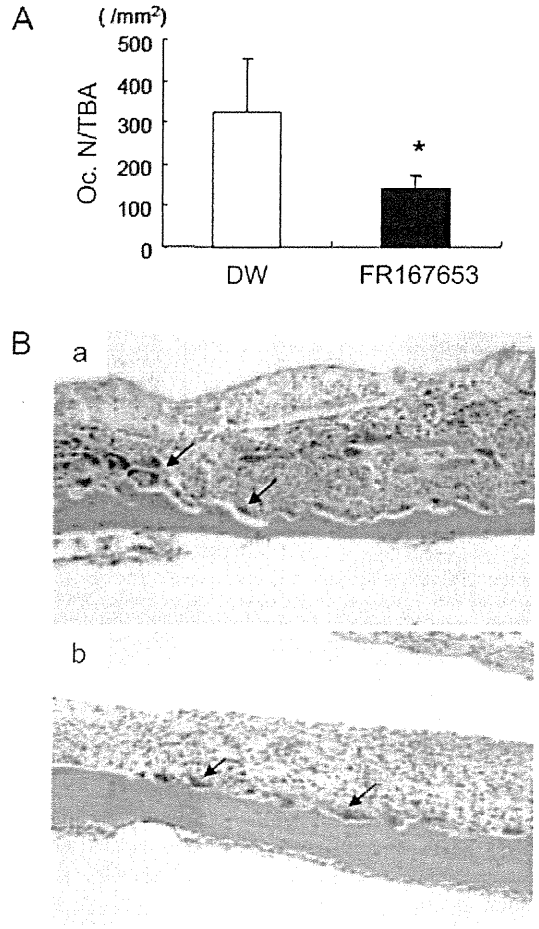

Figure 7. The effects of FR167653 on osteoclast number in calvaria from PTHrP-treated animals. A. Osteoclast number per unit bone area (OcN-BTA) was measured histologically as described in the Materials and Methods section. Treatment of FR167653 reduces the number of osteoclasts (*: P<0.005). B. TRAP staining and counterstain with hematoxylin on calvaria sections. a: Histological section of animals treated with DW. b: Histological section of animals treated with FR167653. Osteoclasts are indicated by arrowheads.
doi:10.1371/journal.pone.0023199.g007

regulation of RANKL and down-regulation of OPG gene expression as mediated by osteoblast or bone marrow stromal cells [25,29]. In our study, however, even the highest concentration of FR167653 that was tested (10 μM) has no effect on RANKL and OPG expression by PTHrP-stimulated primary bone marrow stromal cells. These data suggest that p38 MAPK is not involved in the regulation of PTHrP-mediated bone resorption-related functions of osteoblasts, including regulation of RANKL and OPG expression. This is consistent with previous results that SB203580 has no effect on RANKL and OPG expression by primary osteoblast stimulated with 1α, 25- $(OH)_2D_3$ and PGE_2 [14]. Together, the data suggest that p38 MAPK is involved in the differentiation of osteoclast precursors, rather than in the function of supporting cell such as osteoblasts or bone marrow stromal cells.

However, the current study found that the up-regulation of c-Fos and NFATc1expression treated with RANKL in osteoclast precursor cells (MDBMMs) were inhibited by FR167653 in a dose-dependent manner in both mRNA and protein levels. This strongly suggested the inhibition of osteoclast differentiation by FR167653 is involved in regulating c-Fos and NFATc1 expression in osteoclast precursor cells. The similar results were reported by using SB203580 [30]. These findings, together with the present study, suggest that p38 MAPK-mediated signal propagation down to c-Fos and NFATc1 are of fundamental importance for the differentiation of osteoclast precursors into osteoclasts.

In our animal experiments, local injection of PTHrP on calvaria caused significant bone resorption and systemic hypercalcemia, and increased osteoclast number. Treatment with FR167653 successfully reduced bone resorption and osteoclast number in calvaria, and eventually protected the calvaria from serious osteoclastic dystruction induced by locally administered PTHrP. However, some relieving effect on hypercalcemia was observed. In our hands, inhibition of p38 MAPK by FR167653 significantly decreased the whole-blood calcium level on day 3. However, there is no difference in blood calcium level between the FR167653 treatment group and the control group at day 5.

It was reported that recombinant human OPG is effective in inhibiting bone resorption and hypercalcemia induced by PTHrP *in vivo* [27]. Treatment with chimeric form of OPG in combination with PTHrP (20 μg/day) maintained whole blood ionized calcium

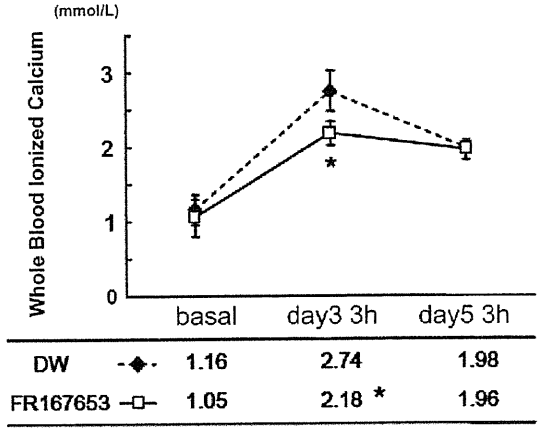

Figure 8. The effect of FR167653 on whole-blood ionized calcium levels in PTHrP-treated mice. PTHrP induces a significant elevation of whole-blood ionized calcium levels in mice within three hours of injection with PTHrP (at day three and five). The whole-blood ionized calcium levels are lower in the FR167653-treated group than in the DW-treated group (control group) at day three (*: $P<0.05$). By day five, however, there was no significant difference between two groups.
doi:10.1371/journal.pone.0023199.g008

levels within the normal range (~1.20 mmol/l). Even though FR167653 was given subcutaneously, it should have act systemically. The concentration of calcium in extracellular fluids is under control by a complex homeostatic system strictly that includes the parathyroid glands, kidneys, bones, and intestines [31,32]. An increase of extracellular calcium concentration is sensed by a calcium-sensing receptor (CaR) in the plasma membrane of parathyroid gland cells and the kidney which in turn affects parathyroid hormone, calcitonin, and 1, 25 (OH) $_2D_3$ secretion. Although intracellular signaling systems regulated by the CaR are still in obscurity, recent evidence suggests that MAPK pathways are activated by CaR [33,34]. For example, calcium homeostasis by angiotensin II in adrenal glomerulosa cells is mediated by activation of p38 MAPK pathways [35]. These observations may help us to understand the surprisingly small effect of p38 MAPK pathway blockade on regulating hypercalcemia induced by PTHrP because the inhibition of p38 MAPK pathway may block CaR signaling pathway as well, which in turn causes reduced reaction to extracellular Ca^{2+} in tissues that express CaR. The detailed mechanism for why inhibition of p38 MAPK partially prevents hypercalcemia even though it is effective in reducing bone resorption merits further studies.

FR167653 has been used in several inflammatory disease models and no obvious adverse events were observed [15–19]. In our previous *in vivo* study [23], we found no significant side effects with daily treatments of 32 mg/kg, a dose found to be safe and effective in other inflammation models as well [36]. In the present study, we also found that there is no significant side effects when twice daily treatment with 30 mg/kg FR167653 for about 1 week. Long-term injection of FR167653 may lead to toxic events; indeed, one study demonstrated that FR167653 treatment increased plasma creatine and lactate dehydrogenase levels in rats [37]. Clearly, the potentially adverse effects of FR167653, including its modulation of calcium homeostasis, need to be studied extensively.

In conclusion, our data indicate that a potent p38 MAPK inhibitor, FR167653, blocks PTHrP-induced osteoclastogenesis *in vitro*, and bone resorption and hypercalcemia *in vivo*. Our results indicate that the responses of other tissues or organs to the p38 MAPK inhibitor may affect calcium homeostasis. This study provides a plausible explanation and target for PTHrP-induced osteoclastogenesis, which will help us to understand the mechanism of bone resorption-related diseases.

Acknowledgments

We thank Dr. Noriyuki Tsumaki for his helpful discussion. We also thank Miss Kanae Asai and Miss Mizuki Nakata for their excellent technical assistance.

Author Contributions

Conceived and designed the experiments: AM. Performed the experiments: HT. Analyzed the data: HT. Contributed reagents/materials/analysis tools: MO. Wrote the paper: MN.

Reference

1. Wysolmerski JJ, Broadus AE (1994) Hypercalcemia of malignancy: the central role of parathyroid hormone-related protein. Annu Rev Med 45: 189–200.
2. Guise TA, Yin JJ, Taylor SD, Kumagai Y, Dallas M, et al. (1996) Evidence for a causal role of parathyroid hormone-related protein in the pathogenesis of human breast cancer-mediated osteolysis. J Clin Invest 98: 1544–1549.
3. Yin JJ, Selander K, Chirgwin JM, Dallas M, Grubbs BG, et al. (1999) TGF-beta signaling blockade inhibits PTHrP secretion by breast cancer cells and bone metastases development. J Clin Invest 103: 197–206.
4. Mundy GR, Yoneda T (1998) Bisphosphonates as anticancer drugs. N Engl J Med 339: 398–400.
5. Coleman RE, Lipton A, Roodman GD, Guise TA, Boyce BF, et al. (2010) Metastasis and bone loss: advancing treatment and prevention. Cancer Treat Rev 36: 615–620.
6. Thomas RJ, Guise TA, Yin JJ, Elliott J, Horwood NJ, et al. (1999) Breast cancer cells interact with osteoblasts to support osteoclast formation. Endocrinology 140: 4451–4458.
7. Lacey DL, Timms E, Tan HL, Kelley MJ, Dunstan CR, et al. (1998) Osteoprotegerin ligand is a cytokine that regulates osteoclast differentiation and activation. Cell 93: 165–176.
8. Yasuda H, Shima N, Nakagawa N, Yamaguchi K, Kinosaki M, et al. (1998) Osteoclast differentiation factor is a ligand for osteoprotegerin/osteoclastogenesis-inhibitory factor and is identical to TRANCE/RANKL. Proc Natl Acad Sci U S A 95: 3597–3602.
9. Kong YY, Yoshida H, Sarosi I, Tan HL, Timms E, et al. (1999) OPGL is a key regulator of osteoclastogenesis, lymphocyte development and lymph-node organogenesis. Nature 397: 315–323.
10. Jimi E, Furuta H, Matsuo K, Tominaga K, Takahashi T, et al. (2011) The cellular and molecular mechanisms of bone invasion by oral squamous cell carcinoma. Oral Dis 17: 462–468.
11. Bucay N, Sarosi I, Dunstan CR, Morony S, Tarpley J, et al. (1998) osteoprotegerin-deficient mice develop early onset osteoporosis and arterial calcification. Genes Dev 12: 1260–1268.
12. Anandarajah AP (2009) Role of RANKL in bone diseases. Trends Endocrinol Metab 20: 88–94.
13. Matsumoto M, Sudo T, Saito T, Osada H, Tsujimoto M (2000) Involvement of p38 mitogen-activated protein kinase signaling pathway in osteoclastogenesis mediated by receptor activator of NF-kappa B ligand (RANKL). J Biol Chem 275: 31155–31161.
14. Li X, Udagawa N, Itoh K, Suda K, Murase Y, et al. (2002) p38 MAPK-mediated signals are required for inducing osteoclast differentiation but not for osteoclast function. Endocrinology 143: 3105–3113.
15. Yamamoto N, Sakai F, Yamazaki H, Nakahara K, Okuhara M (1996) Effect of FR167653, a cytokine suppressive agent, on endotoxin-induced disseminated intravascular coagulation. Eur J Pharmacol 314: 137–142.
16. Yamamoto N, Sakai F, Yamazaki H, Sato N, Nakahara K, et al. (1997) FR167653, a dual inhibitor of interleukin-1 and tumor necrosis factor-alpha, ameliorates endotoxin-induced shock. Eur J Pharmacol 327: 169–174.
17. Takahashi S, Keto Y, Fujita T, Uchiyama T, Yamamoto A (2001) FR167653, a p38 mitogen-activated protein kinase inhibitor, prevents Helicobacter pylori-induced gastritis in Mongolian gerbils. J Pharmacol Exp Ther 296: 48–56.
18. Cau J, Favreau F, Zhang K, Febrer G, de la Motte GR, et al. (2009) FR167653 improves renal recovery and decreases inflammation and fibrosis after renal ischemia reperfusion injury. J Vasc Surg 49: 728–740.
19. Yoshinari D, Takeyoshi I, Koibuchi Y, Matsumoto K, Kawashima Y, et al. (2001) Effects of a dual inhibitor of tumor necrosis factor-alpha and interleukin-1 on lipopolysaccharide-induced lung injury in rats: involvement of the p38 mitogen-activated protein kinase pathway. Crit Care Med 29: 628–634.

20. Nishikori T, Irie K, Suganuma T, Ozaki M, Yoshioka T (2002) Anti-inflammatory potency of FR167653, a p38 mitogen-activated protein kinase inhibitor, in mouse models of acute inflammation. Eur J Pharmacol 451: 327–333.
21. Furuichi K, Wada T, Iwata Y, Sakai N, Yoshimoto K, et al. (2002) Administration of FR167653, a new anti-inflammatory compound, prevents renal ischaemia/reperfusion injury in mice. Nephrol Dial Transplant 17: 399–407.
22. Hou Z, Yanaga K, Kamohara Y, Eguchi S, Tsutsumi R, et al. (2003) A new suppressive agent against interleukin-1beta and tumor necrosis factor-alpha enhances liver regeneration after partial hepatectomy in rats. Hepatol Res 26: 40–46.
23. Nishikawa M, Myoui A, Tomita T, Takahi K, Nampei A, et al. (2003) Prevention of the onset and progression of collagen-induced arthritis in rats by the potent p38 mitogen-activated protein kinase inhibitor FR167653. Arthritis Rheum 48: 2670–2681.
24. Azuma Y, Kaji K, Katogi R, Takeshita S, Kudo A (2000) Tumor necrosis factor-alpha induces differentiation of and bone resorption by osteoclasts. J Biol Chem 275: 4858–4864.
25. Huang H, Chang EJ, Ryu J, Lee ZH, Lee Y, et al. (2006) Induction of c-Fos and NFATc1 during RANKL-stimulated osteoclast differentiation is mediated by the p38 signaling pathway. Biochem Biophys Res Commun 351: 99–105.
26. Boyce BF, Aufdemorte TB, Garrett IR, Yates AJ, Mundy GR (1989) Effects of interleukin-1 on bone turnover in normal mice. Endocrinology 125: 1142–1150.
27. Morony S, Capparelli C, Lee R, Shimamoto G, Boone T, et al. (1999) A chimeric form of osteoprotegerin inhibits hypercalcemia and bone resorption induced by IL-1beta, TNF-alpha, PTH, PTHrP, and 1, 25(OH)2D3. J Bone Miner Res 14: 1478–1485.
28. Matsumoto M, Sudo T, Maruyama M, Osada H, Tsujimoto M (2000) Activation of p38 mitogen-activated protein kinase is crucial in osteoclastogenesis induced by tumor necrosis factor. FEBS Lett 486: 23–28.
29. Brandstrom H, Jonsson KB, Ohlsson C, Vidal O, Ljunghall S, et al. (1998) Regulation of osteoprotegerin mRNA levels by prostaglandin E2 in human bone marrow stroma cells. Biochem Biophys Res Commun 247: 338–341.
30. Horwood NJ, Elliott J, Martin TJ, Gillespie MT (1998) Osteotropic agents regulate the expression of osteoclast differentiation factor and osteoprotegerin in osteoblastic stromal cells. Endocrinology 139: 4743–4746.
31. Magno AL, Ward BK, Ratajczak T (2011) The calcium-sensing receptor: a molecular perspective. Endocr Rev 32: 3–30.
32. Brown EM, MacLeod RJ (2001) Extracellular calcium sensing and extracellular calcium signaling. Physiol Rev 81: 239–297.
33. Tfelt-Hansen J, MacLeod RJ, Chattopadhyay N, Yano S, Quinn S, et al. (2003) Calcium-sensing receptor stimulates PTHrP release by pathways dependent on PKC, p38 MAPK, JNK, and ERK1/2 in H-500 cells. Am J Physiol Endocrinol Metab 285: E329–337.
34. Morgan R, Fairfax B, Pandha HS (2006) Calcium insensitivity of FA-6, a cell line derived from a pancreatic cancer associated with humoral hypercalcemia, is mediated by the significantly reduced expression of the Calcium Sensitive Receptor transduction component p38 MAPK. Mol Cancer 5: 51.
35. Startchik I, Morabito D, Lang U, Rossier MF (2002) Control of calcium homeostasis by angiotensin II in adrenal glomerulosa cells through activation of p38 MAPK. J Biol Chem 277: 24265–24273.
36. Wada T, Furuichi K, Sakai N, Iwata Y, Yoshimoto K, et al. (2000) A new anti-inflammatory compound, FR167653, ameliorates crescentic glomerulonephritis in Wistar-Kyoto rats. J Am Soc Nephrol 11: 1534–1541.
37. Gardiner SM, Kemp PA, March JE, Bennett T (1999) Influence of FR167653, an inhibitor of TNF-alpha and IL-1, on the cardiovascular responses to chronic infusion of lipopolysaccharide in conscious rats. J Cardiovasc Pharmacol 34: 64–69.

JOURNAL OF TISSUE ENGINEERING AND REGENERATIVE MEDICINE
J Tissue Eng Regen Med (2011)
Published online in Wiley Online Library (wileyonlinelibrary.com) **DOI:** 10.1002/term.460

RESEARCH ARTICLE

Feasibility and limitations of the round robin test for assessment of *in vitro* chondrogenesis evaluation protocol in a tissue-engineered medical product

Masako Yokoi[1], Koji Hattori[2], Koichi Narikawa[2], Hajime Ohgushi[3], Mika Tadokoro[3], Kazuto Hoshi[4], Tsuyoshi Takato[4], Akira Myoui[5], Katsuhiko Nanno[5], Yukio Kato[6], Masami Kanawa[6], Katsura Sugawara[7], Tomoko Kobo[7] and Takashi Ushida[1]*

[1]*Centre for Disease Biology and Integrative Medicine (CDBIM), Graduate School of Medicine, University of Tokyo, Japan*
[2]*Department of Orthopaedic Surgery, Nara Medical University, Japan*
[3]*Health Research Institute, National Institute of Advanced Industrial Science and Technology, Hyogo, Japan*
[4]*Division of Tissue Engineering, University of Tokyo Hospital, Japan*
[5]*Medical Centre for Translational Research, Osaka University Hospital, Japan*
[6]*Department of Dental and Medical Biochemistry, Graduate School of Biomedical Sciences, Hiroshima University, Japan*
[7]*Japan Tissue Engineering Co. Ltd, Aichi, Japan*

Abstract

Tissue-engineered medical products (TEMPs) should be evaluated before implantation. Therefore, it is indispensable to establish evaluation protocols in regenerative medicine. Whether or not such evaluation protocols are reasonable is generally verified through a round robin test. However, the round robin test for TEMPs intrinsically includes a deficiency, because identical specimens can not be prepared for TEMPs. The aim of the study was to assess the feasibility and limitations of the round robin test for TEMPs by using a prepared evaluation protocol. We adopted tissue-engineered cartilage constructs as delivered specimens and a protocol of measuring sGAG content as an evaluation protocol proposed to ISO TC150/SC7, which is an invasive, but usually applied, method, although non-invasive methods are keenly required in evaluating TEMPs. The results showed that: (a) the coefficient of variation (CV) of the measured sGAG contents in intralaboratory tests was ~5% at most; (b) the CV of sGAG content in the scheme where each participating laboratory measured different constructs was comparable with that in the scheme where each participating laboratory measured one half of a construct along with the organizing laboratory; (c) the CV caused by factors other than the specimen was ~15%, comparable to that in reproducible experiments in biomedical fields. Based on these results, the study concludes that a round robin test for a TEMP could be valuable, under the condition that the delivered TEMPs are sufficiently reproducible so that the CV of the measured values is <5% in the organizing laboratory. Copyright © 2011 John Wiley & Sons, Ltd.

Received 28 July 2010; Revised 14 January 2011; Accepted 11 June 2011

1. Introduction

Regenerated tissues *in vitro* have a specific feature as a product, i.e. that the tissues are not made by mass production but are those tailor-made, whether their cell sources are autologous or allogenic. This feature means that regenerated tissues are not uniform in their specifications, such as the degree of tissue regeneration, and biochemical and mechanical properties. Therefore, it is necessary to develop specific protocols for evaluating the specifications of each regenerated tissue in a quantitative manner.

The International Organization for Standardization (ISO) is a well-known non-governmental organization

*Correspondence to: T. Ushida, Laboratory of Regenerative Medical Engineering, Centre for Disease Biology and Integrative Medicine (CDBIM), Graduate School of Medicine, University of Tokyo, 7-3-1 Hongo, Bunkyo-ku, Tokyo 113–0033, Japan.
E-mail: ushida@m.u-tokyo.ac.jp

that sets standards. ISO is composed of more than 200 Technical Committees (TCs) to cover a wide range of diverse industrial fields. However, there is no specific TC for tissue-engineered medical products. In 2007, the first subcommittee, SC7, was established in *TC 150, Implants for Surgery*, which discusses standards for tissue-engineered medical products. In September 2007, we submitted to SC7 of TC150 a tentative protocol for Quantification of sulphated glycosaminoglycans (sGAG) for evaluation of chondrogenesis (see Appendix 1). This protocol is an invasive one, although non-invasive methods are keenly required in evaluating TEMPs. However, we adopted this invasive protocol as the protocol in this round robin test because the principal protocols composing this protocol are considered sufficiently reproducible according to a number of published articles.

Whether or not the proposed protocol is reasonable is to be verified through a round robin test. Generally, the round robin test is performed by multiple independent units, using equivalent specimens under the same protocol. However, the same specimens can not be prepared in tissue-engineered medical products (TEMPs). Therefore, the round robin test for TEMPs intrinsically includes a deficiency in this regard.

The present study is the first in which a round robin test for a tissue-engineered medical product has been carried out. Seven independent laboratories participated in the round robin test, using not same but equivalent tissue-engineered cartilage constructs under the above-mentioned protocol. All constructs were prepared by the organizing laboratory. Then we set the following two schemes to deliver the constructs to the participating laboratories. The first scheme was to deliver a whole construct to each participating laboratory; the other was to deliver a cut half-construct to each laboratory – the other half-constructs were measured in the organizing laboratory in the latter case. The present study was designed to assess the feasibility and limitations of the round robin tests of TEMPs through statistical analysis of the sGAG data of all participating laboratories.

2. Materials and methods

2.1. Scheme for protocol evaluation

Tissue-engineered cartilage constructs were prepared at the organizing laboratory (Laboratory of Regenerative Medical Engineering, Centre for Disease Biology and Integrative Medicine, Graduate School of Medicine, University of Tokyo, Japan). The organizing laboratory prepared two types of constructs, the first one using 300 μl collagen gel and the other using 1000 μl collagen gel, which were divided into two halves and delivered to each participating laboratory without any information about sGAG contents. The contents were also measured by the organizing laboratory for each construct (Figures 1a, b, 2a, b). The participating laboratories included: (1) The Centre for Disease Biology and Integrative Medicine (CDBIM), Graduate School of Medicine, University of Tokyo, Japan (organizing laboratory); (2) Department of Orthopaedic Surgery, Nara Medical University, Nara, Japan; (3) Health Research Institute, National Institute of Advanced Industrial Science and Technology, Hyogo, Japan; (4) Division of Tissue Engineering, University of Tokyo Hospital, Japan; (5) Medical Centre for Translational Research, Osaka University Hospital, Japan; (6) Department of Dental and Medical Biochemistry, Graduate School of Biomedical Sciences, Hiroshima University, Japan; (7) Japan Tissue Engineering Co. Ltd, Aichi, Japan.

The sGAGs of the constructs were quantified at each participating laboratory using the protocol Quantification of sulphated glycosaminoglycans (sGAG) for evaluation of chondrogenesis (ISO/TC 150/SC 7/WG3; Appendix 1). The reagents used in the protocol were prepared in each laboratory. All data obtained at each laboratory were reported to the organizing laboratory and statistically analysed in the organizing laboratory.

2.2. Chondrocyte isolation and preparation of tissue-engineered cartilage constructs

Slices of the articular cartilage were harvested under sterile conditions from the knees and shoulder joints of calves (4–8 weeks old), washed twice in Dulbeccos phosphate-buffered saline (PBS) supplemented with 4% antibiotics–antimycotics (10 000 U/ml penicillin, 10 mg/ml streptomycin, and 25 μg/ml amphotericin B; Invitrogen, Grand Island, NY, USA) and minced. The minced cartilage tissue pieces were digested overnight at 37 °C in Dulbeccos modified Eagles medium (DMEM; Invitrogen) supplemented with 10% fetal bovine serum >(FBS; Invitrogen), 0.2% collagenase (CLS II; Worthington, NJ, USA) and 2% antibiotics–antimycotics (Miyata *et al.*, 2004, 2006). The digested solution was filtered through a sterile 70 μm nylon mesh (Cell Strainer, Becton Dickinson Labware, Franklin Lakes, NJ, USA) to remove the debris. The chondrocytes were isolated from the digestion solution by centrifugation and resuspended in the feed medium (DMEM supplemented with 10% FBS, 30 μg/ml L-ascorbic acid and 1% antibiotics–antimycotics). The number of isolated chondrocytes was then counted using a haemocytometer.

Each chondrocyte suspension was mixed with a four-fold volume of 3% atelocollagen solution (Koken, Tokyo), so that the final cell density in the gel was 2.0×10^6 cells/ml (Katsube *et al.*, 2000; Kino-Oka *et al.*, 2005, 2008). A 300 μl or a 1000 μl aliquot of the mixture was placed in a 100 mm diameter culture dish and allowed to gel in a CO_2 incubator for 1 h at 37 °C.

The gels were overlaid with 20 ml culture medium containing 30 μg/ml L-ascorbic acid and 1% antibiotics–antimycotics,

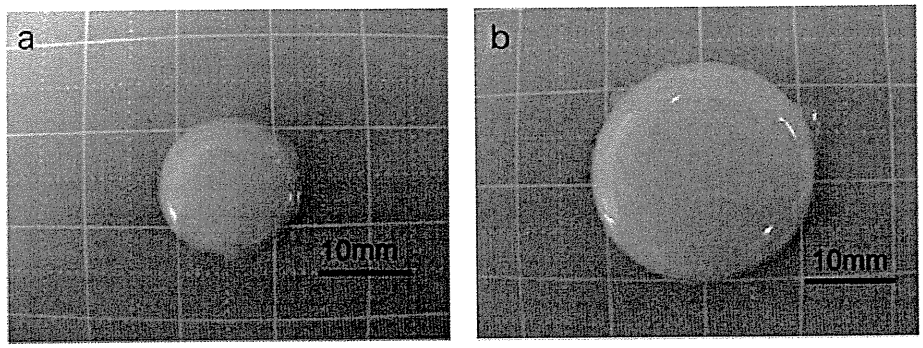

Figure 1. (a) 300 μl gel; (b) 1000 μl gel

and cultured in a 5% CO_2 incubator at 37°C for 2 weeks, with the medium replaced every 3–4 days. Those gels cultured for 2 weeks were delivered to the laboratories as tissue-engineered cartilage constructs for the round robin test.

2.3. Quantification of sGAG in tissue-engineered cartilage constructs

For the constructs of 300 μl gels, each participating laboratory quantified sGAG contents in one whole construct, while the organizing laboratory quantified that in four whole constructs. For the constructs of 1000 μl gels, eight constructs were divided into two halves. In six of these, sGAG content was quantified in each half by the organizing laboratory and in the other half by the other participating laboratories. The sGAG contents of the four halves from the remaining two constructs of 1000 μl gels were quantified by the organizing laboratory.

The constructs (the whole 300 μl gel batch and half of the 1 000 μl gel batch) were placed in 35 mm diameter culture dishes sealed with parafilm, and sent to the participating laboratories under cold conditions. Each participating laboratory measured the sGAG content of both constructs according to the protocol, selecting the dissection method among the options for pretreatment of tissue-engineered cartilage constructs and the papain digestion method among the options for extraction of sGAG from the constructs throughout this round robin test. Every participating laboratory selected either micro-titre plates or cuvettes, according to the equipment available in the 1, 9-dimethylmethylene blue (DMMB) measurement step.

2.4. Statistical analysis

Values were expressed as mean ± SD. Differences between groups were examined for statistical significance using the unequal variance or equal variance *t*-test as a parametric test and Mann–Whitneys U-test as a non-parametric test. $p < 0.05$ was considered statistically significant.

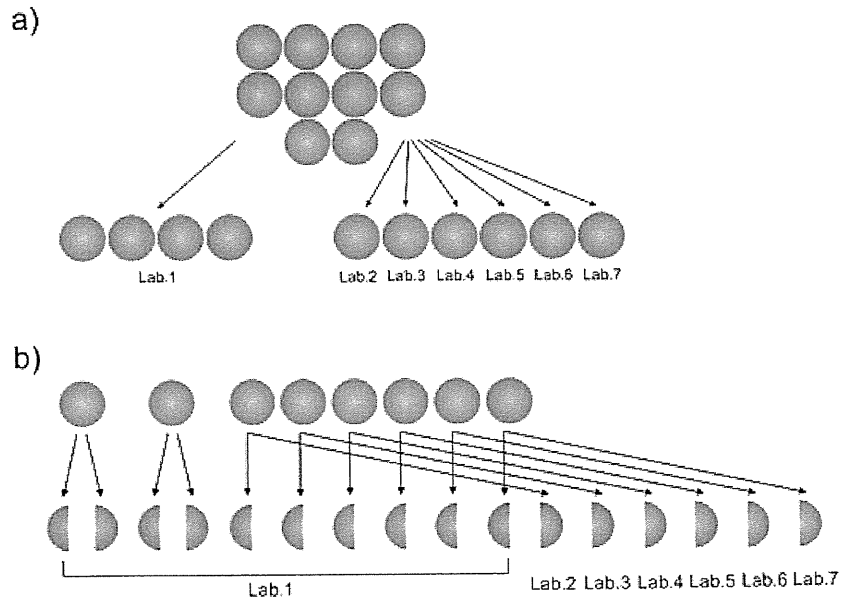

Figure 2. (a) A whole construct of 300 μl gel was delivered to each participating laboratory. (b) 1000 μl gel was divided into two halves, which were delivered to each participating laboratory and organizing laboratory

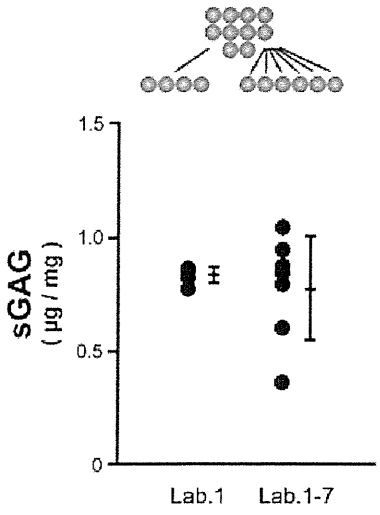

Figure 3. Intra- and interlaboratory variations of sGAG quantification for 300 μl gel. Of 10 300 μl gels, four were quantified for sGAG contents in laboratory 1 and six gels in laboratories 2–7. Circles represent data from laboratories 1–7

3. Results

3.1. Quantification of sGAG contents and intra- and interlaboratory variations in the 300 μl gel constructs

The organizing laboratory quantified the sGAG contents of four 300 μl gel constructs, while the other participating laboratories also quantified the sGAG of one 300 μl gel construct. Figure 3 shows all data of sGAG contents, the mean (M) and standard deviation (SD) values for sGAG contents of the constructs of 300 μl gels determined by the organizing laboratory and participating laboratories. The intralaboratory (organizing laboratory) and interlaboratory coefficients of variation (CVs), which were defined as the ratio of the standard deviation (SD) to the mean (M), were 4.8% and 30%, respectively. Table 1 shows the equipment used to measure the absorbance of the sGAG dye reaction and the correlation coefficients for each standard curve. As the F-test between Lab. 1 and Labs 1–7 showed that the variance in Lab. 1 was not equal to that in Labs 1–7, the unequal variance *t*-test between Lab. 1 and Labs 1–7 was done as a parametric test. The result showed that no significant difference was found between the means in Lab. 1 and Labs 1–7, under the condition that the statistical analysis was done with the limited number of experiments. In the case of biochemical experiments using equivalent samples under the same protocol, normal distribution is generally supposed. However, as the sample numbers were relatively small in this round robin test, we also adopted the Mann–Whitney U-test as a non-parametric test for testing whether two population means are equal or not, because it does not make any assumptions related to the distribution. The result also showed that no significant difference was found between the means in Lab. 1 and Labs 1–7.

3.2. Quantification of sGAG contents and intra- and interlaboratory variations in 1000 μl gel constructs

The organizing laboratory quantified the sGAG contents of 10 halves of the 1000 μl gel constructs, and the other participating laboratories also each quantified the sGAG of a half of a 1000 μl gel construct. Figure 4 shows all the data of sGAG contents, the mean and SD values of the sGAG contents of the 1000 μl gel half-constructs measured by the organizing laboratory and the participating laboratories. The intralaboratory (organizing laboratory) and interlaboratory CVs were 4.4% and 18%, respectively. Table 2 shows equipment used to measure the absorbance of the sGAG dye reaction and the correlation coefficients for the standard curves. As the F-test between Lab. 1 and Labs 1–7 showed that the variance in Lab. 1 was not equal to that in Labs 1–7, the unequal variance *t*-test between Lab. 1 and Labs 1–7 was done as a parametric test. The result showed that no significant difference was found between the means in Lab. 1 and Labs 1–7, under the condition that the statistical analysis was done with the limited number of experiments. We also adopted the Mann–Whitney U-test as a non-parametric test for the 1000 μl gel constructs. This result also showed that no significant difference was found between the means in Lab. 1 and Labs 1–7. Figure 5 shows all data, mean and SD values of the ratios of sGAG contents. Each ratio was calculated by dividing the sGAG content of half of the construct measured at the participating laboratory by that of the other half of the identical construct in the organizing laboratory. The CV of the ratios was 20%. One participating laboratory (Lab. 7) quantified the sGAG contents of the 300 and 1000 μl gel constructs using the Blyscan kit, which is a commercially available kit, based on the same measurement principles as the protocol used in this round robin test, using the spectroscopical shift of DMMB by binding sGAG. The measured values (0.86 and 0.71 μg/mg, respectively) were comparable to those measured by the protocol adopted in

Table 1. Quantification of sGAG contents in the laboratories for 300 μl gel

Quantification laboratory no.	1 (organizing laboratory)				2	3	4	5	6	7
Equipment[a]	M	M	M	M	C	C	C	M	C	M
R^{2b}	0.99	0.99	0.99	0.99	0.93	0.99	0.97	0.98	0.99	0.98

[a]Equipment used to measure absorbance of sGAG dye-reaction. M, microtitre plate reader; C, spectrophotometer using cuvette.
[b]Correlation coefficient for the standard curve.

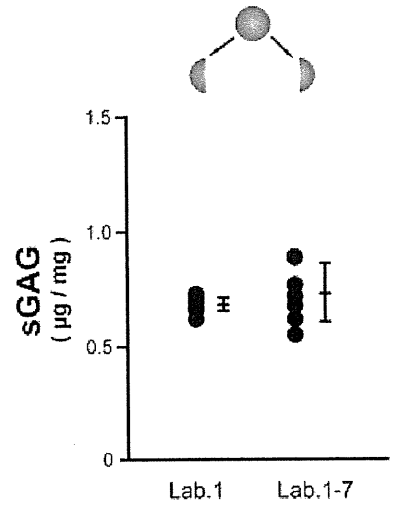

Figure 4. Intra- and interlaboratory variations of sGAG quantification for 1000μl gel. Each of 10 1000μl gels was divided into two halves. Each half was quantified by the organizing laboratory (laboratory 1) and the other half was quantified by the participating laboratories (laboratories 1–7). Circles represent data from laboratories 1–7

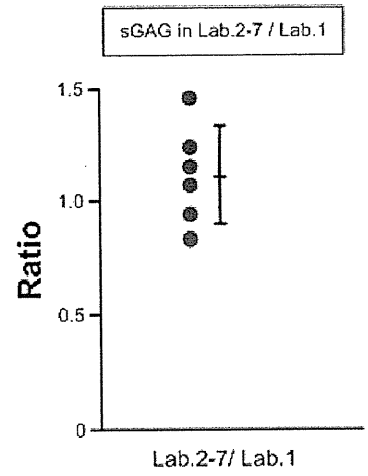

Figure 5. Interlaboratory variation of quantification of the same gels. Circles represent data from laboratories 2–7. For interlaboratory 2–7 variation of the ratio, the data for sGAG contents by laboratory 1 were not used

this round robin test. However, the kit contains solutions all contents of which are not disclosed. Therefore, it does not seem adequate for the standard protocol to include the usage of such kinds of kit. Three laboratories used a microtitre plate reader (M), while four laboratories used spectrophotometers with cuvettes (C). As F-tests between M and C in both the 300 and 1000μl gel constructs showed that the variance in M was equal to that in C, the equal variance *t*-tests between M and C in both constructs were done as a parametric test. The results showed that no significant difference was found between the means in M and C. The same results were obtained using a Mann–Whitney U-test as a non-parametric (one-sided) test.

4. Discussion

4.1. Reliability of the proposed protocol

The protocol used in our round robin test was composed of three major steps, pretreatment, extraction of sGAG and measurement of sGAG content. In the first step, the protocol presents three options, pulverization, lyophilization and dissection. We selected dissection for the pretreatment of the tissue-engineered cartilage constructs throughout this round robin test, because the dissection was a simple and realistic method for pretreating a soft tissue such as the construct used in this round robin test. In the second step, the protocol presents three options, papain digestion, collagenase digestion and guanidine salt extraction. We selected papain digestion for extraction of sGAG from the constructs throughout this round robin test. The papain digestion is a well-known and established method for the digestion of tissue-engineered cartilages (Grande *et al.*, 1997; Hoemann *et al.*, 2002; Kim *et al.*, 1988) and was selected as the most adequate digestion method in this study. We also noted that all constructs prepared in the present study could be digested overnight at 60°C without any debris. The sGAG measurement method in the last step is based on the DMMB assay, which measures the shift in the absorbance profile of the DMMB by binding sGAG. The DMMB assay is widely used for the measurement of sGAG contents (Dey *et al.*, 1992; Farndale *et al.*, 1982, 1986; Stone *et al.*, 1994). Therefore, we concluded that the data generated from the protocol used in our round robin test are reproducible, besides the uniformity of constructs and manipulation errors, because the protocol was designed to conjugate the above-mentioned three methods. This is the reason why we used this protocol to assess the feasibility and limitations of the round robin tests of TEMPs. On the other hand, it is clear that more reasonable and efficient methods, including non-invasive ones, in terms of cost and routine working should be further investigated for evaluating chondrogenesis.

Table 2. Quantification of sGAG content in the laboratories for 1000μl gel

Gel	1000-1		1000-8		1000-2		1000-3		1000-4		1000-5		1000-6		1000-7	
Quantification laboratory no.	1	1	1	1	2	1	3	1	4	1	5	1	6	1	7	1
Equipment[a]	M		M		C	M	C	M	C	M	M	M	C	M	M	M
R^{2b}	0.99	0.99	0.99	0.99	0.93	0.99	0.99	0.99	0.97	0.99	0.98	0.99	0.99	0.99	0.98	0.99

[a]Equipment used to measure absorbance of sGAG dye reaction. M, microtitre plate reader; C, spectrophotometer using cuvette.
[b]Correlation coefficient for the standard curve.

4.2. Uniformity of constructs prepared and delivered in the round robin test

All constructs were generated by one researcher in the organizing laboratory, by mixing suspended bovine chondrocytes with collagen solution as homogeneously as possible. The CVs of sGAG contents of the 300 and 1000 μl gels were 4.8% and 4.4%, respectively, in the organizing laboratory. These CVs correspond with those originated by the protocol and the construct. Then, the CVs of sGAG contents of both gels could be evaluated to be about 5%, if the CV related to the protocol is negligibly low. The results emphasize that the round robin tests of TEMPs intrinsically contain a variance in uniformity of the delivered products, which corresponded to about 5% in this test.

4.3. Interlaboratory variations of measured sGAG contents of the constructs

The interlaboratory CV of sGAG contents of the constructs of 300 μl gels was 30%, although the intralaboratory one was 4.8%. The former CV could be considered relatively large, taking into account that the CVs in reproducible experiments in the biomedical field are generally < 15% (Food and Drug Administration, 2001). Since the intralaboratory CV was 4.8%, the interlaboratory CV could be mainly due to variations of manipulation rather than those of constructs. The same discussion could be developed in the case of the constructs of 1000 μl gels, where the intra- and interlaboratory CVs of sGAG content were 4.4% and 18%, respectively.

The round robin test was conducted with the participation of seven laboratories experienced in measuring sGAG contents. However, it is unlikely that any laboratory could measure sGAG contents of the delivered samples without manipulation errors. It is found that the OD value of 0 μg/ml in the standard curve of Lab 2 was extremely high (0.88 in the raw data). The CVs in 300 μl, 1000 μl and the ratio were recalculated by eliminating the data of Lab 2, resulting in 18%, 19% and 21%, respectively. As far as the recalculated CVs are considered, the CVs in this round robin test were comparable with those in the ordinary round robin tests.

4.4. Estimation of reliability and feasibility of the protocol deduced by the results of the round robin test

The aim of the study was to assess the feasibility and limitations of the round robin tests of TEMPs through two kinds of statistical analysis of the sGAG data obtained by all participating laboratories. The variations in the measured sGAG contents by the round robin test could be due to the following four factors, (a) protocol; (b) specimen; (c) manipulation; (d) equipment, where the second factor is specific to the round robin test for a TEMP. In this round robin test, we adopted tissue-engineered cartilage constructs as the delivered specimens, which were thought to be relatively uniform among TEMPs. The intralaboratory CV was about 5%, which could be caused by the protocol and specimens. Therefore, the CV caused by specimen in this test could be estimated as ~5% at most. On the other hand, we used two schemes for the delivery of the constructs to the participating laboratories. To reduce the variation caused by specimen, it is reasonable to measure the sGAG contents of each half-cut of an identical construct at the organizing laboratory and participating laboratories, and calculate the ratio of the sGAG data. However, a preference in the delivery schemes was not found, based on the comparison between the recalculated CVs in the 300 μl constructs and the ratios (1000 μl). As far as this round robin test is concerned, the estimated CV in the 300 μl and 1000 μl constructs and the ratio caused by factors other than specimen is ~15%, if one simply subtracts the CV caused by the specimen (~5% at most) from the recalculated CVs. This means that the reliability and feasibility of a protocol could be assessed under the above-mentioned limited conditions. We therefore conclude, from the results of this first round robin test, that a round robin test for assessing an evaluation protocol of a TEMP could be valuable under the condition that the delivered TEMPs are to be reproducible such that the CV of the measured values among the delivered TEMPs is < 5% in the organizing laboratory.

Acknowledgements

This study was supported in part by the Japan Science and Technology Agency (JST) and the New Energy and Industrial Technology Development Organization (NEDO), Japan. We thank Assistant Professor Shogo Miyata, Keio University, for valuable technical advice.

APPENDIX 1: Quantification of sulphated glycosaminoglycans (sGAG) for evaluation of chondrogenesis

Scope

This proposal aims to quantify sulphated glycosaminoglycans (sGAG), one of the major matrices in articular cartilage, extracted from tissue-engineered cartilage constructs. The quantification of sGAG as well as collagen is ranked as one of the first steps in evaluating chondrogenesis of the constructs. 1,9-Dimethylmethylene blue (DMMB) dye is selected for quantifying sGAG, which is used for that purpose in a worldwide manner. The procedure to quantify sGAG in the constructs comprises the following steps: 1, pretreatment of the constructs; 2, extraction of sGAG using enzymes or extraction medium; 3, preparation of DMMB reagent; 4, DMMB assay.

Intended performance

1. Preparation of sample solutions from tissue-engineered cartilage

1.1. Pretreatment of tissue-engineered cartilage constructs

Select one of the following three options:

Pulverization

1. Weigh the tissue-engineered cartilage constructs.
2. Dissect the constructs into pieces.
3. Freeze and immediately grind the dissected constructs in liquid nitrogen, and store them at −80°C until extraction.

Lyophilization

1. Weigh the tissue-engineered cartilage constructs.
2. Dissect the constructs into pieces.
3. Freeze-dry the dissected constructs.
4. Transfer the dried constructs into a tube each and add 1–2ml cold distilled water.
5. Incubate them at 4°C overnight, then store them at −80°C until extraction.

Dissection

1. Weigh the tissue-engineered cartilage constructs.
2. Dissect the constructs into enough small pieces to be digested in extraction solutions.
3. Transfer the dissected constructs immediately to the extraction steps.

1.2. Extraction of sGAG from pre-treated samples

Select one of the following three options:

Papain digestion

1. Prepare the papain solution [prepare phosphate-buffered saline (PBS) containing 5mM cysteine–HCl and 5mM EDTA–2Na, pH 6.0; store the reagent at 4°C; add papain (125μg/ml) just before use].
2. Digest pretreated constructs in the papain solution at 60°C overnight. Volume of solution should be determined so that sGAG concentration is measurable in this assay.

Collagenase digestion

1. Prepare collagenase solution (culture medium containing 2.5mg/ml collagenase, 3mM $CaCl_2$ and 0.25% trypsin).
2. Incubate the pretreated constructs with nine times the volume of the collagenase solution at 37°C overnight.

Guanidine salt extraction

1. Prepare 100ml GuCl extraction buffer (4M GuCl, 50mM Tris–HCl, pH 7.5, 1mM EDTA) according to the following procedure: add 38.2g guanidine HCl with 80ml distilled water, 5ml 1M Tris–HCl, pH 7.5, and 200μl 500mM EDTA. Stir them until completely dissolved. Top up the reagent to 100ml with distilled water.
2. Extract pretreated constructs with the GuCl extraction buffer at 4°C overnight.

2. Measurement of sGAG content of extracted solutions

2.1. Preparation of 1,9-dimethylmethylene blue (DMMB) reagent

1. Add 16mg 1,9-dimethylmethylene blue dye to 5ml ethanol, and stir the reagent in a clean dry beaker wrapped with aluminium foil.
2. Add 3.04g glycine, 2.37g NaCl and 95ml 0.1 N HCl to the above reagent.
3. Adjust pH of the reagent to 3.0 with 0.1 N HCl.
4. Top up the reagent to 1000ml with distilled water.
5. Stir the reagent with a magnetic stir bar for 2–16h under shading conditions.
6. Filtrate the reagent with adequate filter paper to removing the debris.
7. Store the reagent in a brown bottle at room temperature, and prepare the reagent freshly every 3months.

2.2. DMMB assay

1. Prepare chondroitin 6-sulphate standard by dissolving 10.0mg chondroitin 6-sulphate with 20ml PBS to make 0.5mg/ml chondroitin 6-sulphate solution, and mix them for several minutes to fully dissolve.
2. Generate a series of chondroitin 6-sulphate solutions in PBS so that the chondroitin 6-sulphate concentrations are 6.25, 12.5, 25, 50 and 100μg/ml, to make a standard curve.
3. Mix 0.1ml each extract or standard solution with 1ml DMMB reagent in a cuvette assay, or mix 0.02ml each extract or standard solution with 0.2ml DMMB reagent in a microtitre plate assay.
4. Measure immediately (within 3min after mixing) the absorbances of the mixtures at 530 (range 525–535) nm.

2.3. Normalization of sGAG contents

1. Convert the absorbance of the mixtures to sGAG concentrations (μg/ml).
2. Normalize the sGAG concentrations (μg/ml) to sGAG contents (μg/mg) by dividing them by the wet weight of the constructs:

sGAG content (μg/ml) $= A$ (μg/ml) $\times B \times (C+D)$ (ml)$/E$ (mg) where A = sGAG concentration (μg/ml), B = dilution rate, C = added digestion volume (ml), D = wet weight of the construct (ml; density of construct is to be 1g/ml) and E = wet weight of the construct (mg).

DOI: 10.1002/term

Bibliography to appendix

ASTM F 2150–07. Standard guide for characterization and testing of biomaterial scaffolds used in tissue engineered medical products. ASTM: West Conshohocken, PA, USA.

ASTM F2312–04. Standard terminology relating to tissue engineered medical products. ASTM: West Conshohocken, PA, USA.

ASTM F2027-00. Standard guide for characterization and testing of substrate materials for tissue engineered medical products. ASTM: West Conshohocken, PA, USA.

ASTM F2210-02. Standard guide for processing cells, tissues, and organs for use in tissue engineered medical products. ASTM: West Conshohocken, PA, USA.

ASTM F2211-04. Standard classification for tissue engineered medical products (TEMPs). ASTM: West Conshohocken, PA, USA.

ASTM F2383-05. Standard guide for assessment of adventitious agents in tissue engineered medical products (TEMPs). ASTM: West Conshohocken, PA, USA.

ASTM F2386-04. Standard guide for preservation of tissue engineered medical products (TEMPs). ASTM: West Conshohocken, PA, USA.

ASTM F2451-05. Standard guide for *in vivo* assessment of implantable devices intended to repair or regenerate articular cartilage. ASTM: West Conshohocken, PA, USA.

Bryant SJ, Aneseth KS. 2002; Hydrogel properties influence ECM production by chondrocytes photoencapsulated in poly(ethylene glycol) hydrogels. *J. Biomed Mater Res* **59**: 63–72.

Chandrasekhar S, Esterman MA, Hoffman HA. 1987; Microdetermination of proteoglycans and glycosaminoglycans in the presence of guanidine hydrochloride. *Anal Biochem* **161**: 103–108.

De Ceuninck H, Sabatini M, Pastoureau P. 2004; Cartilage and Osteoarthritis, vol. 2. Structure and In Vivo Analysis. Methods in Molecular Medicine Series. Humana: New York, NY, USA.

Dey P, Saphos CA, McDonnell J, *et al.* 1992; Studies on the quantification of preteoglycans by the dimethylmethylene blue dye-binding method. Specificity, quantitation in synovial lavage fluid, and automation. *Connect Tissue Res* **28**: 317–324.

Farndale RW, Buttle DJ, Barrett AJ. 1986; Improved quantitation and discrimination of sulphated glycosaminoglycans by use of dimethylmethylene blue. *Biochem Biophys Acta* **883**: 173–177.

Farndale RW, Sayers CA, Barrett AJ. 1982; A direct spectrophotometric microassay for sulfated glycosaminoglycans in cartilage cultures. *Connect Tissue Res* **9**: 247–248.

Grande DA, Halberstadt C, Naughton G, *et al.* 1997; Evaluation of matrix scaffolds for tissue engineering of articular cartilage grafts. *J Biomed Mater Res* **34**: 211–220.

Heinegard D, Sommarin Y. 1987; Isolation and characterization of proteoglycans. *Methods Enzymol* **144**: 319–372.

Hoemann CD, Sun J, Chrzanowski V, *et al.* 2002; A multivalent assay to detect glucosaminoglycans, protein, collagen, RNA, and DNA content in milligram samples of cartilage or hydrogel-based repair cartilage. *Anal Biochem* **300**: 1–10.

ISO 10993–1. Biological evaluation of medical devices – part 1: evaluation and testing. ISO: Geneva, Switzerland.

ISO 10993–19. Biological evaluation of medical devices – part 19: physicochemical, mechanical and morphological characterization. ISO: Geneva, Switzerland.

ISO 14155–1. Clinical investigation of medical devices for human subjects – part 1: general requirements. ISO: Geneva, Switzerland.

ISO 14155–2. Clinical investigation of medical devices for human subjects – part 2: clinical investigation plans. ISO: Geneva, Switzerland.

Kim YJ, Sah RL, Doong JY, *et al.* 1988; Fluorometric assay of DNA in cartilage explants using Hoechst 33258. *Anal Biochem* **174**: 168–176.

Lee CR, Grodzinsky A, Hsu HP, *et al.* 2000; Effects of harvest and selected cartilage repair procedures on the physical and biochemical properties of articular cartilage in the canine knee. *J Orthop Res* **18**: 790–799.

Stone J, Akhtar N, Botchway S, *et al.* 1994; Interaction of 1,9-dimethylmethylene blue with glycosaminoglycans. *Ann Clin Biochem* **31**: 147–152.

References

Dey P, Saphos CA, McDonnell J *et al.* 1992; Studies on the quantification of proteoglycans by the dimethylmethylene blue dye-binding method. Specificity, quantitation in synovial lavage fluid, and automation. *Connect Tissue Res* **28**: 317–324.

Farndale RW, Sayers CA, Barrett AJ. 1982; A direct spectrophotometric microassay for sulfated glycosaminoglycans in cartilage cultures. *Connect Tissue Res* **9**: 247–248.

Farndale RW, Buttle DJ, Barrett AJ. 1986; Improved quantitation and discrimination of sulphated glycosaminoglycans by use of dimethylmethylene blue. *Biochem Biophys Acta* **883**: 173–177.

Food and Drug Administration (FDA). 2001; Guidance for Industry: Bioanalytical Method Validation. FDA: Silver Spring, MD, USA.

Grande DA, Halberstadt C, Naughton G *et al.* 1997; Evaluation of matrix scaffolds for tissue engineering of articular cartilage grafts. *J Biomed Mater Res* **34**: 211–220.

Hoemann CD, Sun J, Chrzanowski V *et al.* 2002; A multivalent assay to detect glycosaminoglycan, protein, collagen, RNA, and DNA content in milligram samples of cartilage or hydrogel-based repair cartilage. *Anal Biochem* **300**: 1–10.

Katsube K, Ochi M, Uchio Y *et al.* 2000; Repair of articular cartilage defects with cultured chondrocytes in atelocollagen gel: comparison with cultured chondrocytes in suspension. *Arch Orthop Trauma Surg* **120**: 121–127.

Kim YJ, Sah RL, Doong JY *et al.* 1988; Fluorometric assay of DNA in cartilage explants using Hoechst 33258. *Anal Biochem* **174**: 168–176.

Kino-Oka M, Yashiki S, Ota Y *et al.* 2005; Subculture of chondrocytes on a collagen type I-coated substrate with suppressed cellular dedifferentiation. *Tissue Eng* **11**: 597–608.

Kino-Oka M, Maeda Y, Sato Y *et al.* 2008; M. Characterization of spatial growth and distribution of chondrocyte cells embedded in collagen gels through a stereoscopic cell imaging system. *Biotechnol Bioeng* **99**: 1230–1240.

Miyata S, Furukawa K, Ushida T *et al.* 2004; Static and dynamic mechanical properties of extracellular matrix synthesized by cultured chondrocytes. *Mater Sci Eng C* **24**: 425–429.

Miyata S, Homma K, Numano T *et al.* 2006; Assessment of fixed charge density in regenerated cartilage by Gd–DTPA-enhanced MRI. *Magn Reson Med Sci* **5**: 73–78.

Stone J, Akhtar H, Botchway S *et al.* 1994; Interaction of 1,9-dimethylmethylene blue with glycosaminoglycans. *Ann Clin Biochem* **31**: 147–152.

Leukemia Research 35 (2011) 1205–1211

Contents lists available at ScienceDirect

Leukemia Research

journal homepage: www.elsevier.com/locate/leukres

Predictability of the response to tyrosine kinase inhibitors via *in vitro* analysis of Bcr-Abl phosphorylation

Masaru Shibata[a], Sachiko Ezoe[a,*], Kenji Oritani[a], Keiko Matsui[a], Masahiro Tokunaga[a], Natsuko Fujita[a], Yuri Saito[a], Takayuki Takahashi[b], Masayuki Hino[c], Itaru Matsumura[d], Yuzuru Kanakura[a]

[a] *Hematology and Oncology, Osaka University, Graduate School of Medicine, 2-2 Yamada-oka, Suita, Osaka 565-0871, Japan*
[b] *Kobe City Medical Center General Hospital, Kobe, Japan*
[c] *Department of Hematology, Graduate School of Medicine, Osaka City University, Osaka, Japan*
[d] *Department of Internal Medicine, Kinki University School of Medicine, Sayama, Japan*

ARTICLE INFO

Article history:
Received 16 December 2010
Received in revised form 12 January 2011
Accepted 14 January 2011
Available online 26 March 2011

Keywords:
CML
Tyrosine kinase inhibitor
Bcr-Abl
Crkl
Phosphorylation
Immunoblot

ABSTRACT

It would be of great value to predict the efficacy of tyrosine kinase inhibitors (TKIs) in the treatment of individual CML patients. We propose an immunoblot system for detecting the phosphorylation of Crkl, a major target of Bcr-Abl, in blood samples after *in vitro* incubation with TKIs. When the remaining phosphorylated Crkl after treatment with imatinib was evaluated as the "residual index (RI)", high values were found in accordance with imatinib resistance. Moreover, RI reflected the outcome of imatinib- as well as second generation TKIs with a high sensitivity and specificity. Therefore, this system should be useful in the selection of TKIs.

1. Introduction

The introduction of tyrosine kinase inhibitors (TKIs) targeting Bcr-Abl have dramatically improved the treatment of CML. Imatinib mesylate (Gleevec; Novartis Pharmaceuticals, East Hanover, NJ) was shown to induce high rates of cytogenetic and molecular responses, resulting in greatly prolonged survival in CML patients [1,2]. However, despite the remarkable improvement in survival and responsiveness with imatinib-treatment, a considerable proportion of the patients treated with imatinib have been reported to exhibit either primary or secondary resistance or intolerance [3–5]. Clinical resistance to imatinib can result from mutations in the Abl kinase domain at residues that directly contact imatinib or that influence imatinib binding [6]. As resistance can also arise in the absence of Bcr-Abl mutations, other mechanisms of resistance and disease progression may exist, including Bcr-Abl-independent signaling in CML cells [7]. To overcome the resistance and intolerance to imatinib, efforts have been made to develop second- and third-generation TKIs. Examples of such inhibitors include nilotinib (Tasigna, Novartis) [8], dasatinib (Sprycel, Bristol-Myers Squibb) [9] and other TKIs under clinical investigation such as bosutinib [10] and INNO-406 [11]. These TKIs are significantly more potent than imatinib and have exhibited efficacy against many types of imatinib-resistant Bcr-Abl mutants. Furthermore, they are also candidates for first-line therapy, as there is a need to improve the results achieved with imatinib [12–14]. In parallel with the entrance of new therapeutic compounds, an important question is which TKI is the most appropriate to each CML patient.

To establish a system with which we can predict the response of each patient to TKIs, we investigated in this study the phosphorylation of Crkl, a major target of Bcr-Abl, after *in vitro* incubation with or without TKIs in peripheral blood (PB) samples from patients either newly diagnosed or resistant to imatinib. It is demonstrated that this *in vitro* analysis system is highly reflective of the clinical response to TKIs of CML patients, and these data should prove useful in selecting TKIs in individual cases.

2. Patients, materials and methods

2.1. Patient blood samples

Thirty-one patients with CML in the chronic phase (CP) were included in this study (Table 1). The optimal response, response and resistance were defined in accordance with the European Leukemia Net (ELN) recommendations [15,16]. Briefly, an "optimal response" to imatinib means achieving a complete hematological response (CHR) at 3 months or complete cytogenetic response (CCyR) at

* Corresponding author. Tel.: +81 6 6879 3871; fax: +81 6 6879 3879.
E-mail address: sezoe@bldon.med.osaka-u.ac.jp (S. Ezoe).

0145-2126/$ – see front matter © 2011 Elsevier Ltd. All rights reserved.
doi:10.1016/j.leukres.2011.01.012

6 months after the induction of imatinib, and resistance means failure to achieve such a response. On the other hand, in nilotinib- or dasatinib-treated patients, a "response" means a minor cytogenetic response (mCyR) at 3 months or partial cytogenetic response (PCyR) at 6 months after the induction of the second generation TKI, and resistance means failure to achieve this response.

Ten microliters of the PB samples were obtained from patients with informed consent at the beginning or before the initiation of imatinib, nilotinib or dasatinib. Half of each sample was used for examination of the Bcr-Abl sequence, which was performed by the SRL Co. (Tokyo, Japan), and the other half was used for immunoblot analysis.

Approvals for the study were obtained from the institutional review boards of all the participating facilities.

2.2. Reagents

Imatinib, methanesulfonate salt was kindly provided by Novartis Pharmaceuticals (Basel, Switzerland), and nilotinib and dasatinib were purchased from LC laboratories (Boston, MA). The antibodies used in this study were as follows: anti-Lyn, anti-phospho-Crkl, anti-phospho-c-Abl from Cell Signaling Technology (Beverly, MA), anti-phospho-Lyn(Y396) from Epitomics (Burlingame, CA), anti-Crkl, anti-β-actin from Santa Cruz Biotechnology (Santa Cruz, CA), and the secondary antibodies, anti-Rabbit IgG HRP and anti-Goat IgG HRP were from Promega (Madison, WI). Pervanadate was purchased from Sigma–Aldrich (St. Louis, MO).

2.3. Cell line

A Bcr-Abl positive human cell line, K562, was used in the preliminary experiments in this study. K562 cells were maintained in RPMI1640 (nacalai tesque, Kyoto, Japan) supplemented with 10% fetus bovine serum (FBS) (EQUITECH-BIO, Kerrville, TX).

2.4. Immunoblot assays of patients' samples

Whole blood cell samples from patients were used within 3 h after blood had been drawn. Red cells were lysed with Whole Blood Lysing Reagents (Beckman Coulter, Brea, CA), and white blood cells were cultured with or without imatinib, nilotinib or dasatinib. After 5-h incubation, the cell lysates were collected and subjected to immunoblot assays. Gel electrophoresis and immunoblot assays were performed according to methods described previously [17,18]. Immunoreactive proteins were visualized with an enhanced chemiluminescence detection system (PerkinElmer Life Sciences, Boston, MA).

2.5. Evaluation of phosphorylation intensity and determination of the "residual index (RI)"

The intensity of each blot of immunoreactive protein was quantified using ChemiDoc XRS+ with Image Lab Software (Bio Rad, Tokyo Japan). The RI values of each patient to TKIs were determined in accordance with the numerical expression, as indicated in Fig. 2A.

2.6. Statistical analysis

Analysis of variance was used to assess data reproducibility. The Mann–Whitney rank sum was used to define differences between groups.

3. Results

3.1. Immunoblot analysis of phosphorylated Crkl in CML patients

To assess the drug response of the CML patients, we performed immunoblot assays detecting phosphorylated Crkl, a direct target of Bcr-Abl kinase. To establish the experimental procedures, preliminary experiments were performed with K562, a CML blast crisis cell line, or blood sample from a newly diagnosed CML patient (Patient A), 98% of whose PB cells were Bcr-Abl-positive on fluorescence *in situ* hybridization (FISH). First, to determine the optimum incubation period for the TKIs, PB cells were incubated with or without TKIs for varying time periods. A two-hour incubation was not sufficient because imatinib did not completely suppress the phosphorylation of Crkl, while 24-h incubation was too long because the PB neutrophils appeared to die (Fig. 1A, left panel). A five-hour incubation completely eliminated the phosphorylation of Crkl without cell death. On the other hand, simultaneous treatment with a phosphatase inhibitor sustained the phosphorylation of Crkl even after treatment for 24 h (Fig. 1A, right panel). Thus, we decided to incubate cells for 5 h without phosphatase inhibitors. Next, to build an *in vitro* simulation model for the estimation of the activities of TKIs in the body, we fixed the concentrations of TKIs at the peak value of plasma concentrations in patients (Cmax) after administration of the recommended dose of TKIs. The Cmax of imatinib in CML patients after taking orally 400 mg of the drug is 3.0–4.8 μM, and that of nilotinib after taking 400 mg is 2.9–4.0 μM. In the case of

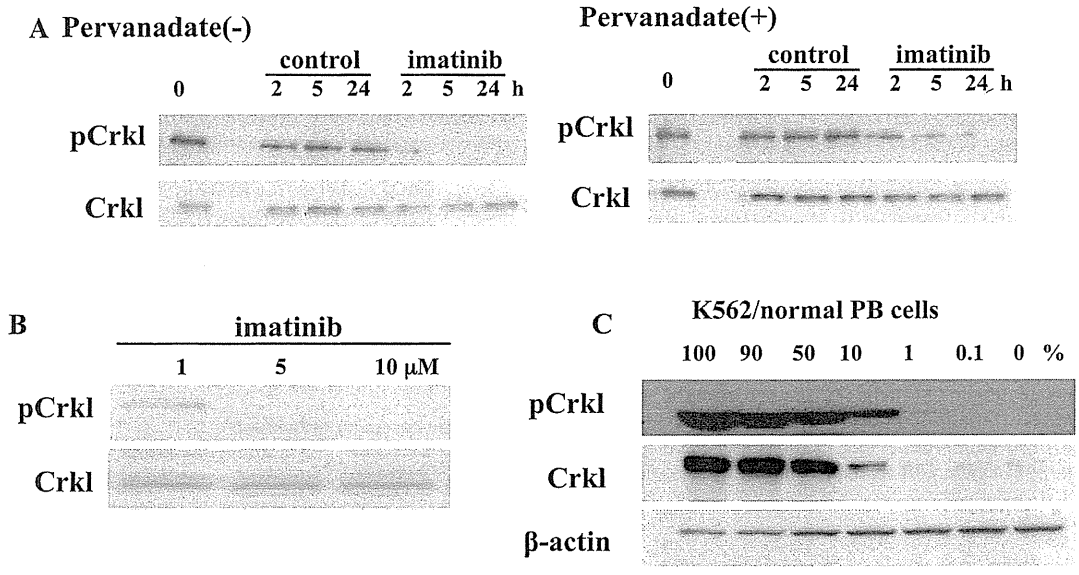

Fig. 1. Optimization of western blot after TKI-incubation. (A and B) Blood sample from Patient A was incubated with or without 5 μM imatinib supplemented with (right panel) or without (left panel) 10 μM of pervanadate for the indicated periods (A) or incubated with imatinib at the indicated concentrations for 5 h (B). The treated cells were lysed and subjective to immunoblot analysis using the indicated antibodies. (C) K562 cells were mixed into normal human PB cells at the indicated ratios. Then the samples were subjective to immunoblot analysis.

dasatinib, the Cmax after the ingestion of 100 mg dasatinib was 100nM [19–21]. In terms of pharmacokinetics, we fixed the concentrations of these TKIs (imatinib, nilotinib and dasatinib) at 5 μM, 5 μM, and 0.1 μM, respectively. As shown in Fig. 1B, 1 μM of imatinib did not eliminate the phosphorylation of Crkl in the examined sample of patient A who are newly diagnosed and well responded to imatinib, but 5 μM and 10 μM of imatinib did, indicating that 1 μM is too low concentration for estimation of clinical outcome. Finally, to estimate the sensitivity of this system, K562 cells were mixed with normal PB cells at variable ratios, as indicated. Fig. 1C shows that the phosphorylated Crkl at the lowest 1% was detectable in K562 cells. Thus, we analyzed patients having more than 10% Bcr-Abl-positive cells in PB by FISH.

3.2. Iimmunoblot analysis

To quantify the *in vitro* responsiveness to TKIs, we measured the density of each blot using a densitometric method. We then defined "residual index (RI)" for each TKI by the numerical expression as shown in Fig. 2A. Triplicate measurements were performed on 3 individual patients (Patient B, C and D). There were no significant variations among the RIs in each patient. Standard error for each sample set was less than 5% (4.6%, 1.2% and 3.4%, respectively) (Fig. 2B).

3.3. Responses to the TKIs in patients with various stages of CML

Fig. 3A represents typical results of the immunoblot analyses in 2 patients with newly diagnosed CML (Patient 1 and 2), and 2 patients who were receiving imatinib but were displaying resistance (Patient 16 and 17). Although all of these samples exhibited apparent phosphorylation of Crkl without TKIs, the phosphorylated Crkl disappeared from the samples of Patients 1 and 2 when incubated with imatinib, nilotinib or dasatinib. In the case of Patients 16 and 17, on the other hand, weak bands remained in the imatinib and/or nilotinib-incubated samples, but disappeared in the dasatinib-treated ones. Thus, this immunoblot analysis appeared to be useful in evaluating Crkl phosphorylation after *in vitro* TKI-incubation. All patients were divided into two groups: one being newly diagnosed and another receiving imatinib-therapy but showing resistance. The imatinib-RIs of the samples from the imatinib-resistant group (median RI: 34.2%) were much higher than those of the samples from newly diagnosed patients (median RI: 4.2%) (Fig. 3B).

3.4. Sequential examinations using the residual index

RI values were analyzed sequentially in the course of the different TKI-treatments in 2 imatinib-resistant patients (Patient 23 and 27).

Patient 23 (Fig. 4A): after six months of treatment with imatinib, the drug was changed to dasatinib because of a failure to achieve an optimal response (72% $Ph1^+$ in FISH). Six months after the start of dasatinib, $Ph1^+$ cells were disappeared. The samples were obtained twice: prior to the treatment with imatinib, and at the time of change to dasatinib. Immunoblot analysis showed that neither imatinib nor nilotinib eliminated the phosphorylation of Crkl at the initiation of treatment, but dasatinib did. Furthermore the RI values were under 10% only in the sample incubated with dasatinib.

Patient 27 (Fig. 4B): when the first sample was obtained, the percentage of $Ph1^+$ cells was 93% after 7-year treatment with imatinib.

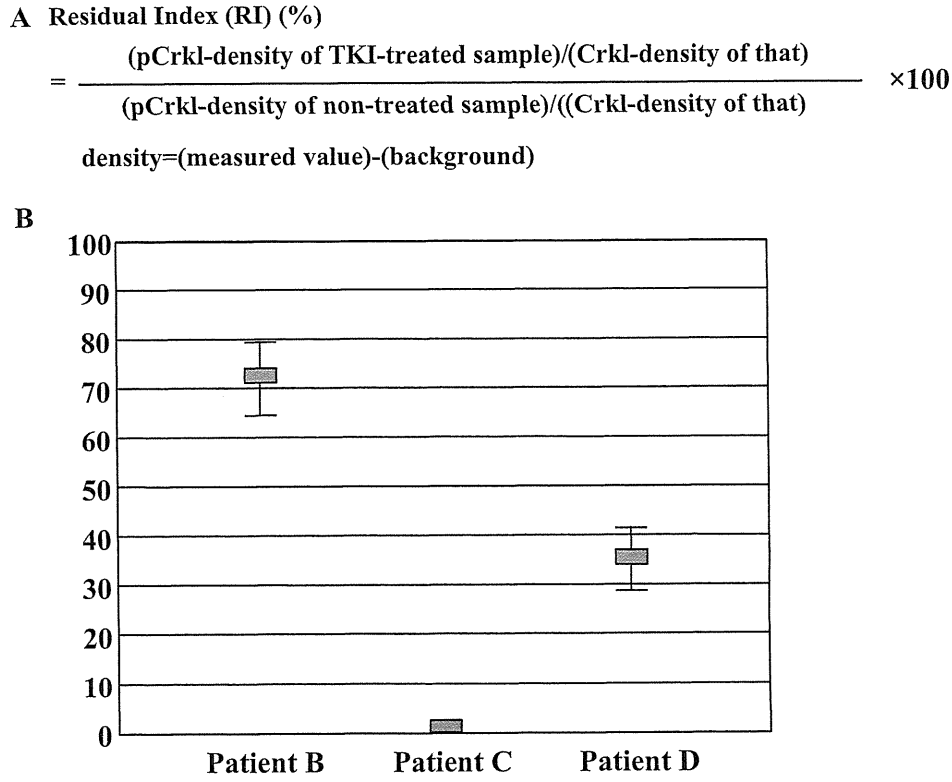

Fig. 2. "Residual index (RI)". (A) The numerical expression of RI. "Measured value" means the density of each blot measured by densitometric method. (B) The reproducibility of RIs for imatinib treatment. Means and standard errors, representing triplicate assays in 3 patients, are shown.

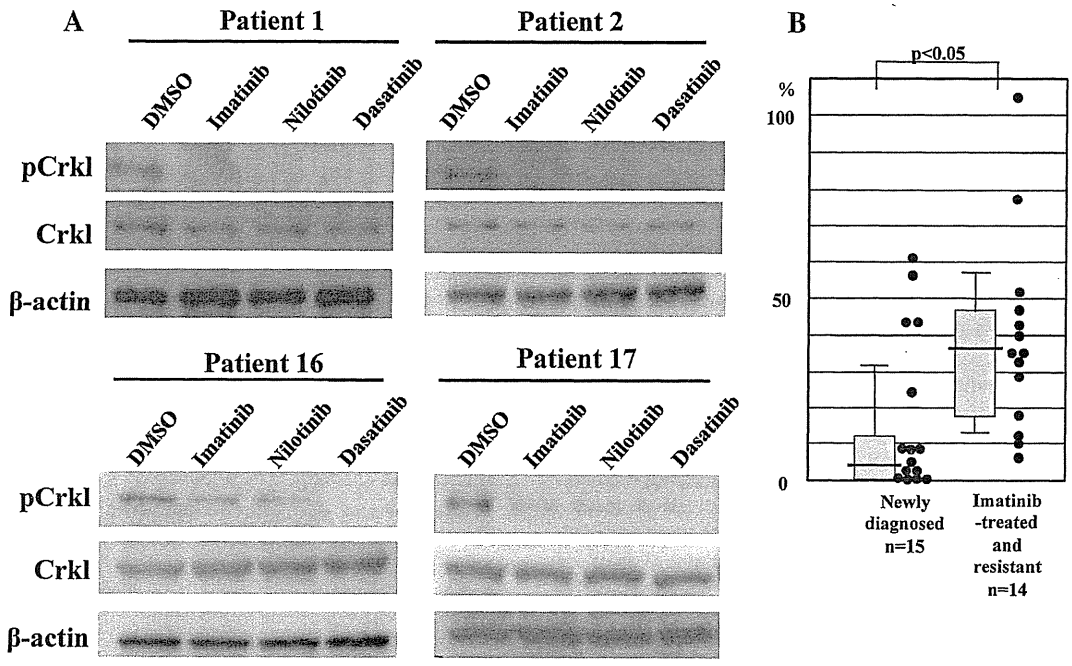

Fig. 3. Different RI values against imatinib between patients at diagnosis and patients showing imatinib-resistance. (A) Four typical data of immunoblots were represented. PB cells from newly diagnosed patients (Patient 1 and 2) or patients (Patient 16 and 17) who had been receiving imatinib-therapy but showed its resistance were incubated for 5 h *in vitro* with or without indicated TKIs. The concentration of imatinib, nilotinib, and dasatinib are 5 μM, 5 μM, and 0.1 μM, respectively. The incubated cells were lysed and subjected to immunoblot analysis using the indicated antibodies. (B) RIs against imatinib were calculated in 15 patients at diagnosis and 14 patients who had been receiving imatinib-therapy and showed its resistance. The distribution of RIs in each group was plotted. Representative box plots show values within the 25th to 75th percentile. Medians are indicated in crossbar. Fifth and 95th percentiles are shown by error bars. The statistical difference was $p < 0.05$.

Then the treatment was changed to dasatinib, which was stopped because of a strong pancytopenia. The patient was then treated with nilotinib, but the percentage of $Ph1^+$ cells again increased. The second sample was obtained at the time of the change from dasatinib to nilotinib. In both samples, the incubation with the three TKIs did not eliminate the phosphorylation of Crkl. Although the second sample exhibited a strong sensitivity only to dasatinib (RI = 4.1%), the remaining CML cells additionally displayed continuous Lyn-phosphorylation (Fig. 4B).

3.5. RIs in patients with Bcr-Abl point mutations

The most important issue in TKIs resistance is the acquisition of point mutations in Bcr-Abl. Bcr-Abl mutations were detected in 4 samples (Table 2). The RI values of Patient 28, with a threonine-to-isoleucine mutation at codon 315 (T315I), were higher than 10% in all the TKI-treated samples. In accordance with the *in vitro* results, the disease was refractory to both imatinib and dasatinib. A phenylalanine-to-leucine mutation at codon 317 (F317L) and a methionine-to-threonine at codon 351 (M351T) were detected in Patient 27. F317L is reported to confer high responsiveness to nilotinib, while M351T does the same to dasatinib. The RI values of this patient were over 10% in all of the samples treated with TKIs, which conformed the outcome of failing to achieve CHR after nilotinib or dasatinib treatment. Next, the RI value in the sample with the phenylalanine-to-valine mutation at codon 359 (F359V) (Patient 23) was less than 10% only in the dasatinib-treated sample, which does not conflict with the reported IC50 data. Finally, although the F317L mutation is reported to be highly sensitive to nilotinib, the RI value for nilotinib in Patient 19, who later proved to be resistant to nilotinib but responded to dasatinib, was higher than 10%, and lower than 10% for dasatinib. Therefore, RIs are likely to be highly correled with the favorability of Bcr-Abl mutations to TKIs, and in some cases, to predict the responsiveness with higher sensitivity than mutations.

3.6. Correlation of RI with patient outcome

To analyze whether the RIs correlate with the clinical response to TKIs, newly diagnosed patients ($n = 15$) were separated into two groups in accordance with the most recent outcome, imatinib-sensitive ($n = 13$), who achieved an optimal response after the sample collection, and imatinib-resistant ($n = 2$), who did not. The median RI of the patients in the sensitive group was 4.2% and that in the resistant group was 43.2% ($p < 0.05$) (Fig. 5, left panel). We also assessed the predictability of the response to nilotinib. Eight patients imatinib resistant had undergone nilotinib-therapy. Among them, 4 achieved optimal responses and the others failed. The median RI in the nilotinib-sensitive group was 3.5% in contrast to 31.2% in the resistant group (Fig. 5, middle panel). Although the sample size was too small to conduct statistical analysis, the RIs were clearly separated between dasatinib-sensitive and -resistant groups (Fig. 5, right panel).

When the cut-off value of RI was set at 10%, the specificities, sensitivities and predicted values were all 100% in terms of nilotinib and dasatinib responsiveness (Table 3). Also, in the evaluation of imatinib-treatment, the specificity and sensitiveness were more than 77%. Therefore, it is suggested that the RIs (cut-off value: 10%) are useful as a novel predictor for clinical utility of TKIs, especially in imatinib-resistant cases.

4. Discussion

Imatinib, the first approved TKI for CML, frequently induces durable cytogenetic remission and thus occupies an important position as the current standard of care. Now, second-generation

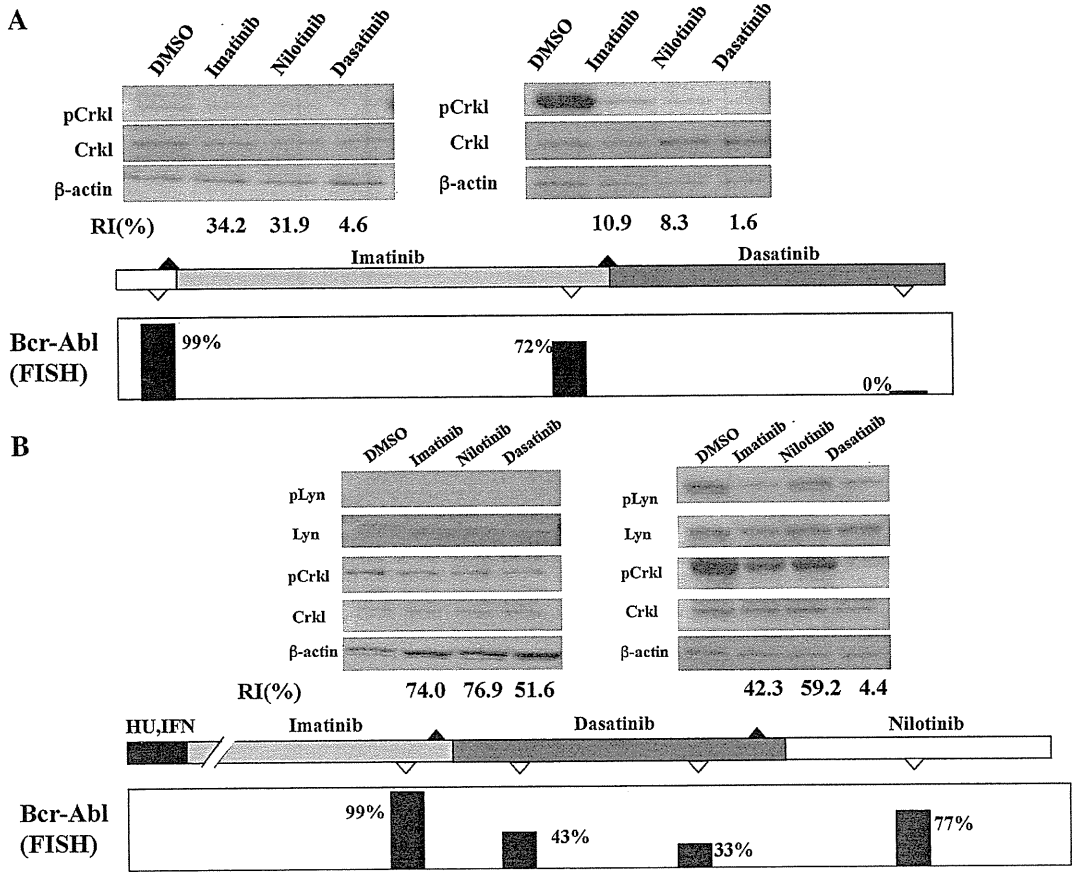

Fig. 4. Sequential examinations of RI values during clinical treatments in two patients. Immunoblots were sequentially analyzed during CML-treatment in two patients who showed resistance to TKIs. Data of immunoblots using the indicated antibodies are shown with their clinical course. FISH analyses are indicated by open triangles, and immunoblot analysis by closed triangles.

Table 1
Patient characteristics.

Characteristic	
No. of patients	31
Median age, y (range)	55 (20–89)
Sex (male/female)	14/17
Treatment before sample collection	
No	13
IFN	3
TKI	18
Bcr-Abl mutation	4
Median follow-up, months (range)	6 (3–14)

TKIs, such as nilotinib and dasatinib, have now been made available [12,13]. Although these TKIs are significantly more potent and show higher sensitivity against some imatinib-resistant mutations, there are no useful guidelines for the proper choice of second-generation TKIs in imatinib-resistant patients. Furthermore, second-generation TKIs have recently been recommended as first-line therapies based on the evidence that an earlier achievement of remission may provide a better clinical outcome or less disease progression. There is still a need for indicators pointing to the proper drug choice for individual patients. The *in vitro* responsiveness to TKIs in terms of cell proliferation has been demonstrated to be a predictor of clinical response. The IC50, a cell based screen for resistance determining the drug concentration that can induce 50% of growth suppression, is a potent predictor of the responsiveness to drugs. In patients with *de novo* CML, the $IC50^{imatinib}$ was reported to possess a high predictive value [22]. However, determination of the IC50 for each TKI requires so much effort and time that an application suitable for all patients may be quite a distant prospect. Furthermore, as the optimal concentration varies for each TKI, comparing the efficacy between different TKIs is difficult. Although the cellular IC50 s for the effect of TKIs on Bcr-Abl point mutations have been reported [23–26], this information

Table 2
Patients with BCR-ABL mutations, and their RI values.

Patient	Mutation	RIs			Clinical outcome
		Imatinib	Nilotinib	Dasatinib	
Patient 19	F317L	40.0	30.8	3.9	Imatinib and nilotinib resistant, and dasatinib respond
Patient 23	F359V	15.8	11.9	1.4	Imatinib resistant, and nilotinib and dasatinib intolerant
Patient 27	M351T/F317L	74.0	76.9	51.6	imatinib resistant, and nilotinib and dasatinib intolerant
Patient 28	T315I	104.2	88.0	93.0	Imatinib and dasatinib resistant

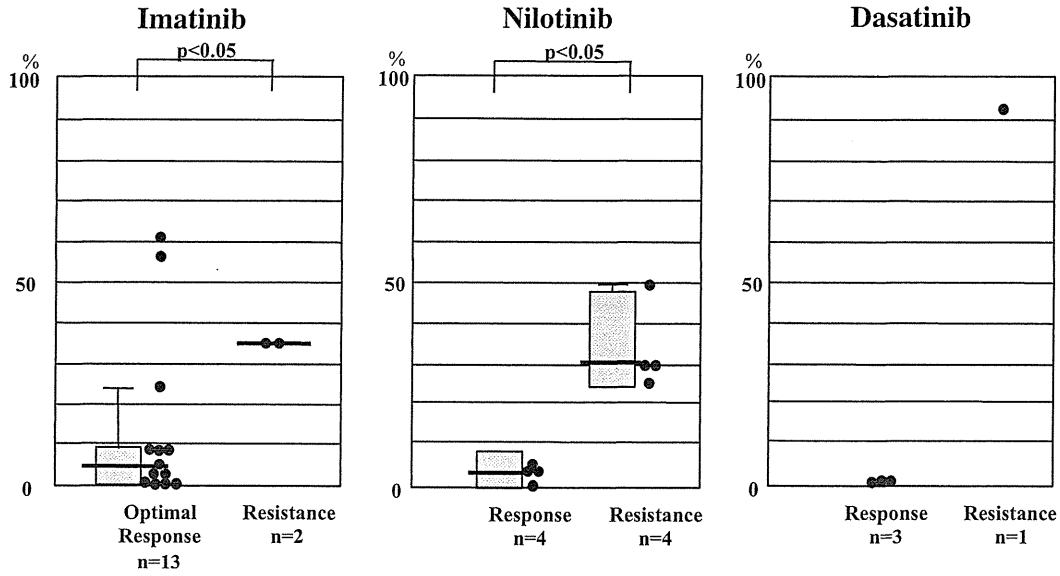

Fig. 5. RI values in patients grouped by clinical response to each TKI-therapy. Fifteen patients were newly diagnosed as CML, and their PB cells were obtained just before the beginning of imatinib-therapy. The patients were divided into two groups: "optimal response" in imatinib-treated patients means *de novo* CML patients who later proved to achieve optimal response, and "Resistance" means patients who later failed to achieve optimal response. Among 12 patients who had showed imatinib-resistance, 8 patients received nilotinib-therapy and 4 patients received dasatinib-therapy at a stretch of imatinib-therapy. Their PB cells were obtained just before the change of therapy. The patients were divided into two groups: that of responsive patients and of resistant patients to each TKI. Dot plots demonstrate the RI values of patients to each TKI. Representative box plots show values within the 25th to 75th percentile. Medians are indicated in crossbar. Fifth and 95th percentiles are shown by error bars.

Table 3
Sensitivity and specificity.

	Optimal response	Resistance	Predicted value
Newly diagnosed and Imatinib-treated patients ($n=15$)			
RI < 10	10	0	100%
RI ≥ 10	3	2	40%
Specificity/sensitivity	77%	100%	
Imatinib-resistant and Nilotinib-treated patient ($n=8$)			
RI<10	4	0	100%
RI ≥ 10	0	4	100%
Specificity/sensitivity	100%	100%	
Imatinib-resistant and Dasatinib-treated patients ($n=4$)			
RI < 10	3	0	100%
RI ≥ 10	0	1	100%
Specificity/sensitivity	100%	100%	

	Newly diagnosed and later achieved optimal response	Imatinib-treated and showed resistance to Imatinib	Predicted value
All included and evaluable patients ($n=27$)			
RI < 10	10	1	91%
RI ≥ 10	3	13	81%
Specificity/sensitivity	77%	93%	

is only useful when the mutated subclone is the predominant cell population.

In this study, we evaluated the effect of TKIs on Crkl phosphorylation as a "residual index". It is noteworthy that the samples from patients who had shown resistance to imatinib had much higher RIs than the samples from newly diagnosed patients. In the case of newly diagnosed patients, most samples responsive to imatinib *in vitro*, but two patients whose samples displayed markedly high RIs *in vitro* proved not to achieve an optimal response to the drug. Although substantial accordance was later detected in the immunoblot data between the responsiveness and resistance to imatinib, a few samples had markedly high RIs in patients who later achieved optimal responses to imatinib. These exceptional cases will have to be followed for a longer period. The data showed 100% of sensitivity and 77% of specificity when the RIs were separated at 10%. On the other hand, in imatinib-resistant patients, the results of the tests did reflect the patient outcome. Although the sample size was small, the immunoblot analysis was able to predict the clinical responsiveness to nilotinib or dasatinib treatment with 100% sensitivity and specificity. Thus, this system can be a useful tool for selecting TKIs, especially in imatinib-resistant patients. It may be inferred that the lower confidence in